

Expanding the genotypic spectrum of Jalili Syndrome: Novel *CNNM4* variants and uniparental isodisomy in a North American patient cohort

Lev Prasov^{1,2,3}, Ehsan Ullah¹, Amy E. Turriff¹, Blake M. Warner⁴, Julie Conley⁵, Paul R. Mark⁶, Robert B. Hufnagel¹, Laryssa A. Huryrn^{1*}

- 1 Ophthalmic Genetics and Visual Function Branch, National Eye Institute, National Institutes of Health, Bethesda, MD 20892
- 2 Department of Ophthalmology, W.K. Kellogg Eye Center, University of Michigan, Ann Arbor, MI 48105
- 3 Department of Human Genetics, University of Michigan, Ann Arbor, MI 48109
- 4 National Institute of Dental and Craniofacial Research, National Institutes of Health, Bethesda, MD 20892
- 5 Section of Pediatric Ophthalmology, Helen DeVos Children's Hospital, Grand Rapids, Michigan 49503
- 6 Spectrum Health Division of Medical Genetics, Grand Rapids, Michigan 49503

* Author for correspondence:

Laryssa A. Huryrn, MD
tel: 301-435-8810
laryssa.huryrn@nih.gov
Building 10, Rm 10D45; 10 Center Dr.
Bethesda, MD 20892

Running Title: Novel *CNNM4* variants in Jalili syndrome

This is the author manuscript accepted for publication and has undergone full peer review but has not been through the copyediting, typesetting, pagination and proofreading process, which may lead to differences between this version and the [Version of Record](#). Please cite this article as doi: [10.1002/ajmg.a.61484](https://doi.org/10.1002/ajmg.a.61484)

ABSTRACT

Jalili syndrome is a rare multisystem disorder with the most prominent features consisting of cone-rod dystrophy and amelogenesis imperfecta. Few cases have been reported in the Americas. Here we describe a case series of patients with Jalili syndrome examined at the National Eye Institute's Ophthalmic Genetics clinic between 2016 and 2018. Three unrelated sporadic cases were systematically evaluated for ocular phenotype and determined to have cone-rod dystrophy with bull's eye maculopathy, photophobia and nystagmus. All patients had amelogenesis imperfecta. Two of these patients had Guatemalan ancestry and the same novel homozygous *CNNM4* variant (p.Arg236Trp c.706C>T) without evidence of consanguinity. This variant met likely pathogenic criteria by the American College of Medical Genetics guidelines. An additional patient had a homozygous deleterious variant in *CNNM4* (c.279delC p.Phe93Leufs*31), which resulted from paternal uniparental isodisomy for chromosome 2p22-2q37. This individual had additional syndromic features including developmental delay and spastic diplegia, likely related to mutations at other loci. Our work highlights the genotypic variability of Jalili syndrome and expands the genotypic spectrum of this condition by describing the first series of patients seen in the United States.

Key Words:

Jalili syndrome
Cone-rod dystrophy

amelogenesis
CNNM4

retinal degeneration
uniparental isodisomy

INTRODUCTION

Jalili syndrome is a rare multisystem disorder characterized by a childhood cone-rod retinal degeneration and amelogenesis imperfecta[Jalili 2010]. It was initially described in a large extended family in Gaza, as an autosomal recessive condition in which all affected family members had photophobia, nystagmus, and achromatopsia along with abnormal tooth enamel[Jalili and Smith 1988]. Since that time, most cases have been described in large consanguineous families on multiple continents, including one family in Newfoundland[Doucette and others 2013] and one family in Guatemala[Parry and others 2009], with few reported sporadic cases[Daneshmandpour and others 2019].

Though variants in many genes can lead to amelogenesis imperfecta or cone-rod dystrophy, the constellation of these two findings in the absence of other syndromic features is highly suggestive of one gene, *CNNM4*, as the underlying cause[Daneshmandpour and others 2019; Parry and others 2009; Polok and others 2009]. *CNNM4* encodes a transmembrane protein with a critical role in magnesium homeostasis, and is expressed in photoreceptors and in the dental enamel[Gomez Garcia and others 2011; Parry and others 2009; Polok and others 2009]. Here, we describe a series of sporadic cases with Jalili syndrome in a cohort of patients originating in North and Central America. These patients carry novel variants in *CNNM4* and further highlight the variable phenotypic and genotypic spectrum of the condition.

METHODS

This study was carried out according to the standards of the Common Rule of the United States Federal Government (46CFR45) under protocols approved by the Institutional Review Board at the National Institutes of Health and all participants provided informed consent. Patients were evaluated in the Ophthalmic Genetics and Visual Function Branch Clinic between 2016 and 2018. All patients underwent ophthalmic clinical evaluation, including best corrected visual acuity (BCVA) using the Early Treatment of Diabetic Retinopathy Study (ETDRS) chart and guidelines, refraction, color vision testing by monocular Farnsworth D15, slit-lamp biomicroscopy, dilated eye exam, Goldmann visual field testing, fundus color and autofluorescence (FAF) imaging (Topcon, Tokyo, Japan; Optos, Dunfermline, Scotland), optical coherence tomography (Cirrus HD-OCT, Carl Zeiss Meditec, Dublin, CA; Bioptigen Inc., Research Triangle Park, NC), electroretinography (ERG) (LKC, Gaithersburg, MD), and medical evaluation by a clinical geneticist. ERGs were recorded using Burian-Allen electrodes and according to the International Society for Clinical Electrophysiology of Vision standards. Ocular, medical and dental health records were also reviewed, including panoramic and bite wing X-rays when available. Patients without molecular results underwent clinical genetic testing with an inherited retinal dystrophy panel (Molecular Vision Laboratory (MVL); Hillsboro, OR; Clinical Laboratory Improvement Amendments identifier,

38D2059762). *CNNM4* variants were evaluated for pathogenicity using established American College of Medical Genetics (ACMG) criteria [Richards and others 2015].

RESULTS

Case Reports

Patient 1

Patient 1 is a 15-year-old girl born from Guatemalan parents who presented with poor central vision, nystagmus, and light sensitivity. Examination was notable for Snellen BCVA at distance of 20/250 in the right eye and 20/200 in the left eye. Auto-refraction showed a myopic refraction with astigmatism: $-2.75+2.25 \times 103$ and $-3.00+3.00 \times 076$ in the right and left eye, respectively. She had high frequency, low amplitude horizontal nystagmus and was orthophoric. Anterior segment exam was unremarkable, and fundus exam was notable for bull's eye maculopathy and granular pigment changes in the periphery. Spectral domain optical coherence tomography (SD-OCT) revealed loss of the ellipsoid zone in the fovea, and FAF demonstrated a bull's eye pattern of hyper- and hypo-autofluorescence (**Figure 1**). Farnsworth D15 color vision testing revealed multiple axis errors (achromatic pattern). Loss of the I1e isopter was noted on the Goldmann visual field testing in each eye, with preservation of I4e and V4e isopters. Scotopic electroretinography showed diminished amplitudes (~50%) and mildly delayed implicit times, while photopic bright flash and flicker ERG responses were unrecordable. The dental examination and dental radiographs (bitewings, anterior

and posterior periapical radiographs, and panoramic radiograph) revealed an entirely restored dentition with crowns on all molar teeth and composite restorations on the anterior teeth (**Figure 2**). The pulp chambers appear slightly enlarged on some teeth (20, 23, 26, 29) while others exhibit appearance within normal limits for this age (**Figure 2, Supplemental Figure 1**). Clinically, the enamel is thin or absent on the non-restored surfaces of the teeth. Periapical and bitewing radiographs reveal isolated residual enamel on non-restored and under restored surfaces, respectively (**Supplemental Figure 1, arrows**). There were otherwise no systemic abnormalities noted. A 581 gene panel from Molecular Vision Lab (MVL Panel v1) revealed a homozygous *CNNM4* c.706C>T (p.Arg236Trp) variant with one copy inherited from each parent.

Patient 2

Patient 2 is a 16-year-old boy from Guatemala, who presented with poor central vision and light sensitivity. Examination was notable for Snellen BCVA at distance of 20/200 in the right eye and 20/160 in the left eye, with a manifest refraction of +1.00+4.50x109 and -0.25+4.25x069, respectively. He had mild end-gaze nystagmus and was orthophoric. Anterior segment exam was unremarkable, and fundus exam was notable for bull's eye maculopathy, perivascular and segmental pigment deposition in the inferior retina, and mild vascular attenuation (**Figure 1A-D**). OCT revealed loss of the ellipsoid zone in the fovea, and FAF imaging revealed a hypofluorescent sector corresponding to the areas of retinal atrophy and pigment deposition. Color vision

testing by Farnsworth D15 revealed multiple axis errors. Goldmann visual fields demonstrated superior constriction, and loss of the I1e isopter centrally, consistent with the retinal changes inferiorly (**Figure 1**). Scotopic ERG showed mildly diminished amplitudes and delayed implicit times, while photopic bright flash and flicker ERG were extinguished. Dental examination revealed crowns on multiple teeth and absence of enamel. There were otherwise no systemic abnormalities. Molecular Vision Lab NGS Retinal Dystrophy SmartPanel v11 (281 genes) revealed a homozygous *CNNM4* c.706C>T (p.Arg236Trp) variant with one copy inherited from each parent.

Patient 3

Patient 3 is a 3-year-old boy born from a Puerto Rican father and Caucasian mother who presented to ophthalmology clinic with light sensitivity and multiple congenital anomalies. On examination, binocular visual acuity was 2.4cy/cm by Teller acuity cards (approximately 20/360 Snellen equivalent). Cycloplegic refraction showed myopia with astigmatism in both eyes: -3.25+2.25x090 and -3.25+2.50x095, in the right and left eye, respectively. Anterior segment exam was unremarkable. Fundus exam was notable for diffuse granular pigment changes and bull's eye maculopathy, with typical corresponding bull's eye pattern on FAF (**Figure 1**). Bioptogen OCT revealed loss of the ellipsoid zone at the fovea (**Figure 1**). Dental examination revealed crowns on multiple molar teeth and yellow/opaque appearance of the anterior teeth with thinning and complete absence of enamel on some teeth (**Figure 2**). Systemic

evaluation was notable for spastic paraplegia, developmental delay, and fatty liver. The patient was dependent on tracheostomy for respiration and gastrostomy tube for feeding. Clinical whole exome sequencing revealed homozygosity for a frameshift variant in *CNNM4*: c.279delC (p.Phe93Leufs*31). Segregation analysis revealed that this variant was present in only the patient's father and not mother. Subsequent analysis examining other single nucleotide polymorphisms (SNPs) revealed paternal uniparental isodisomy (UPD) on chromosome 2p22-2q37. With the exception of homozygosity for the *CNNM4* variant, no additional variants within the UPD region were directly linked to the phenotypic features of the patient.

Genetic analysis

We evaluated pathogenicity of *CNNM4* variants in each patient using established ACMG criteria. The *CNNM4* c.279delC (p.Phe93Leufs*31) creates a frameshift early in the protein, which would be predicted to result in nonsense mediated decay of RNA or generation of a nonfunctional protein. The *CNNM4* c.706C>T (p.Arg236Trp) variant creates a non-conservative substitution in the protein in a highly conserved residue (GERP score 4.99) located in the DUF21 domain of the protein. The missense variant p.Arg236Trp was predicted to be damaging by 14 different in-silico prediction tools (SIFT, PolyPhen2, PROVEAN, DANN, DEOGEN2, EIGEN, FATHMM-MKL, M-CAP, MVP, MutationAssess, MutationTaster, REVEL, MetaSVM, MetaLR) whereas it was predicted benign by only one in-silico tool (PrimateAI)[Kopanos and others 2019]. Also,

the missense variant p.Arg236Trp had a high CADD score[Rentzsch and others 2019] of 32, while the gnomAD missense Z score (2.37) indicates that *CNNM4* gene is moderately constrained against missense changes. The p.Arg236Trp variant was found to be absent in population databases comprised of healthy (gnomAD, <https://gnomad.broadinstitute.org>) as well as diseased individuals (HGMD, <http://www.hgmd.cf.ac.uk>; ClinVar, <https://www.ncbi.nlm.nih.gov/clinvar/>). Notably, limited haplotype analysis on genetic panel data did not reveal additional homozygous variants in *CNNM4* or surrounding genes *ALMS1* and *MERTK* on chromosome 2, suggesting this is a founder mutation in the Guatemalan population rather than a result of consanguinity or previously unknown relatedness between families of patients 1 and 2. A previous variant in this same amino acid, *CNNM4* c.707G>A (p.Arg236Gln), segregated with disease in a large family with Jalili syndrome, with a 0.5^{17} probability of co-segregation by chance [Polok and others 2009]. This variant was also absent from the gnomAD database. Based on 2015 ACMG/AMP variant interpretation criteria, *CNNM4* p.Phe93Leufs*31 is considered pathogenic and p.Arg236Gln is considered likely pathogenic [Richards and others 2015].

DISCUSSION

The phenotypic spectrum of Jalili syndrome typically comprises cone-rod dystrophy and amelogenesis imperfecta, but there is significant variability in the severity of the retinal degeneration, even within families with the same

mutation [Daneshmandpour and others 2019] [Gerth-Kahlert and others 2015; Jalili 2010]. Consistent with this observation, we see a difference in structural and functional measures among two patients of similar age and demographic background carrying the same *CNNM4* p.Arg236Trp variant. While both have significant cone dysfunction and a bull's eye maculopathy, Patient 2 has a significant peripheral sector of retinal atrophy and pigment deposition with a corresponding visual field defect, while Patient 1 has disease mostly limited to the posterior pole. This suggests that factors beyond the genotype influence the disease severity. Both probands were of Guatemalan descent, denied consanguinity, and yet carried the same homozygous variant. This suggests a founder effect, though the ancestor may be more distant as neither patient carries homozygous variants in neighboring retinopathy genes *ALMS1* or *MERTK*, which would constitute a ~39Mb haplotype block. Likewise, the previously reported Guatemalan family carried two different mutations [Parry and others 2009], suggesting that there are at least 3 alleles present in this population.

We report the first case of uniparental isodisomy associated with Jalili syndrome. This patient had additional features including spastic paraplegia, fatty liver, and developmental delay, while both his father and mother were phenotypically normal. Though the patient carried a large stretch of UPD on chromosome 2p22-2q37, complete UPD of chromosome 2 can be tolerated [Ou and others 2013; Zhang and others 2019]. Uniparental isodisomy causes disease by two predominant mechanisms, loss of

heterozygosity uncovering rare deleterious variants and through disruption of imprinting. In our case, a frameshift variant in *CNNM4*, which was paternally inherited, was uncovered and led to the Jalili syndrome phenotype. Exome failed to reveal any rare coding variants that were thought to cause the non-retinal and non-dental phenotypes. Likewise, no imprinting disorders with overlapping features have been described for these regions on chromosome 2. It remains possible that homozygosity for non-coding variants explain the other neurological phenotypes.

Our work describes the detailed phenotypic features of this condition in an underreported patient population, identifies a novel missense variant shared by two of the patients, and highlights an unusual case of UPD leading to the disorder. Future efforts will be necessary to identify the full spectrum of UPD-associated disorders on chromosome 2 and identify the precise cause of the additional features in this patient. Additionally, mechanistic studies exploring the structure and function of the DUF21 domain of *CNNM4* will be necessary to identify the function of this critical portion of the protein.

ACKNOWLEDGEMENTS

The authors are grateful to the individuals and families for participating in the study; to Denise Cunningham, Mike Arango and the ophthalmic photographers and technicians at the National Institutes of Health Ophthalmic Genetics Clinic.

This research was funded by the NEI intramural Research Grant.

The data that support the findings of this study are available from the corresponding author upon reasonable request.

WEB RESOURCES

gnomAD Database: <http://gnomad.broadinstitute.org/>

NCBI Human Reference Genome Build 37.1:

<http://www.ncbi.nlm.nih.gov/genome/assembly/2928/>

Clinvar: <https://www.ncbi.nlm.nih.gov/clinvar/>

HGMD: <http://www.hgmd.cf.ac.uk>

REFERENCES:

- Daneshmandpour Y, Darvish H, Pashazadeh F, Emamalizadeh B. 2019. Features, genetics and their correlation in Jalili syndrome: a systematic review. *Journal of medical genetics* 56(6):358-369.
- Doucette L, Green J, Black C, Schwartzentruber J, Johnson GJ, Galutira D, Young TL. 2013. Molecular genetics of achromatopsia in Newfoundland reveal genetic heterogeneity, founder effects and the first cases of Jalili syndrome in North America. *Ophthalmic genetics* 34(3):119-129.
- Gerth-Kahlert C, Seebauer B, Dold S, Hanson JV, Wildberger H, Sporri A, van Waes H, Berger W. 2015. Intra-familial phenotype variability in patients with Jalili syndrome. *Eye* 29(5):712-716.
- Gomez Garcia I, Oyenarte I, Martinez-Cruz LA. 2011. Purification, crystallization and preliminary crystallographic analysis of the CBS pair of the human metal transporter CNNM4. *Acta crystallographica Section F, Structural biology and crystallization communications* 67(Pt 3):349-353.
- Jalili IK. 2010. Cone-rod dystrophy and amelogenesis imperfecta (Jalili syndrome): phenotypes and environs. *Eye* 24(11):1659-1668.
- Jalili IK, Smith NJ. 1988. A progressive cone-rod dystrophy and amelogenesis imperfecta: a new syndrome. *Journal of medical genetics* 25(11):738-740.
- Kopanos C, Tsiolkas V, Kouris A, Chapple CE, Albarca Aguilera M, Meyer R, Massouras A. 2019. VarSome: the human genomic variant search engine. *Bioinformatics* 35(11):1978-1980.
- Ou X, Liu C, Chen S, Yu J, Zhang Y, Liu S, Sun H. 2013. Complete paternal uniparental isodisomy for Chromosome 2 revealed in a parentage testing case. *Transfusion* 53(6):1266-1269.
- Parry DA, Mighell AJ, El-Sayed W, Shore RC, Jalili IK, Dollfus H, Bloch-Zupan A, Carlos R, Carr IM, Downey LM, Blain KM, Mansfield DC, Shahrabi M, Heidari M, Aref P, Abbasi M, Michaelides M, Moore AT, Kirkham J, Inglehearn CF. 2009. Mutations in CNNM4 cause Jalili syndrome, consisting of autosomal-recessive cone-rod dystrophy and amelogenesis imperfecta. *American journal of human genetics* 84(2):266-273.
- Polok B, Escher P, Ambresin A, Chouery E, Bolay S, Meunier I, Nan F, Hamel C, Munier FL, Thilo B, Megarbane A, Schorderet DF. 2009. Mutations in CNNM4 cause recessive

cone-rod dystrophy with amelogenesis imperfecta. *American journal of human genetics* 84(2):259-265.

Rentzsch P, Witten D, Cooper GM, Shendure J, Kircher M. 2019. CADD: predicting the deleteriousness of variants throughout the human genome. *Nucleic Acids Res* 47(D1):D886-D894.

Richards S, Aziz N, Bale S, Bick D, Das S, Gastier-Foster J, Grody WW, Hegde M, Lyon E, Spector E, Voelkerding K, Rehm HL, Committee ALQA. 2015. Standards and guidelines for the interpretation of sequence variants: a joint consensus recommendation of the American College of Medical Genetics and Genomics and the Association for Molecular Pathology. *Genetics in medicine : official journal of the American College of Medical Genetics* 17(5):405-424.

Zhang X, Ding Z, He R, Qi J, Zhang Z, Cui B. 2019. Complete Paternal Uniparental Disomy of Chromosome 2 in an Asian Female Identified by Short Tandem Repeats and Whole Genome Sequencing. *Cytogenetic and genome research* 157(4):197-202.

FIG LEGENDS:

Figure 1. Ocular features of Jalili syndrome cases. (A-C) Multimodal imaging of the right eye of patient 1: SD-OCT (A) demonstrating ellipsoid zone disruption in the fovea; ring of hyper- hypo-autofluorescence on wide-field Optos autofluorescence (B) and bull's eye maculopathy on 50 degree color fundus photo (C) are all consistent with the cone-rod dystrophy. (D-F) Multimodal imaging of patient 2's left eye showing loss of foveal ellipsoid zone on OCT (D), with hypofluorescent sector of inferior retina on wide-field Optos autofluorescence (E), corresponding to the areas of atrophy and retinal pigment migration on color fundus photo (F). (G-I) Multimodal imaging of patient 3's right eye showing macular changes on Bioptogen OCT (G), with corresponding bull's eye hyper- hypo-autofluorescence pattern on wide-field Optos autofluorescence (H),

and diffuse granular pigment changes and bull's eye maculopathy on wide-field Optos color photograph (I).

All patients share bull's eye maculopathy, with loss of ellipsoid and interdigitation zone as evidenced by the hyporeflective dark area under the fovea on OCT. However, patient 2 also notably has a large hypoautofluorescent area of atrophy and pigment clumping in the periphery (E,F).

Figure 2. Dental features of Jalili syndrome cases. (A-B) External photos of mouth of patient 1 (A) and patient 3 (B) showing tooth decay and crowns on multiple teeth. (C) Panoramic X-ray of patient 1 showing crowns on all adult molar teeth.

Supplemental Figure 1. Periapical radiographs of the maxillary (A) and mandibular (B) teeth and bitewing radiographs of the right (C) and left (D) occlusal plane. These radiographs demonstrate the restorative state of the teeth and illustrate that the enamel is almost entirely lost in this patient (more radiopaque appearance denoted by the arrows). Only minimal enamel remains (arrows), typically under stainless steel crown coverage or interproximal areas with minimal wear. The radiographs also reveal the irregularities in pulp and root canal shape with some teeth demonstrating slightly enlarged pulp chambers while others are more typical and some have sclerotic appearing root canals.

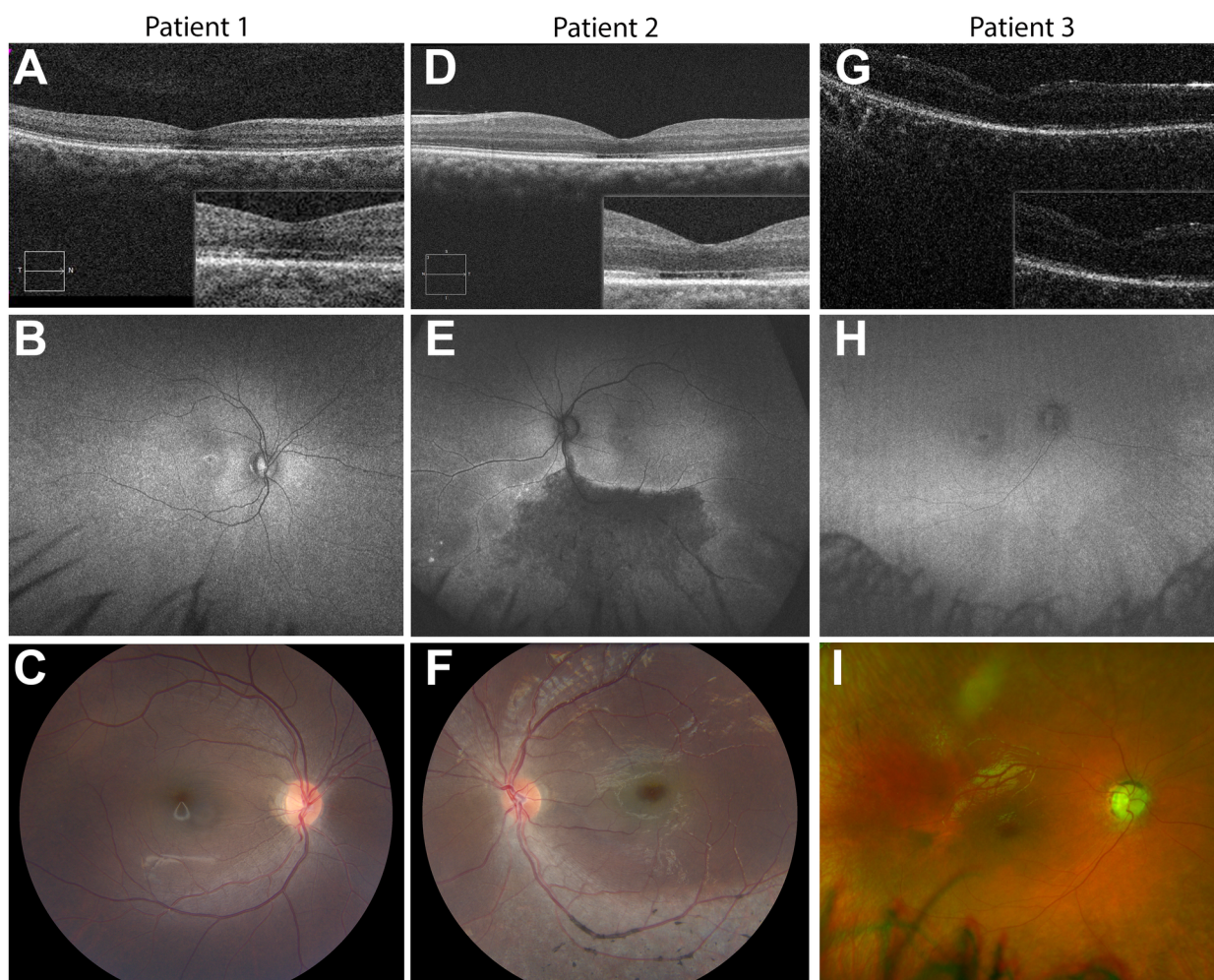


Figure1-fundusphotos-v2.tif

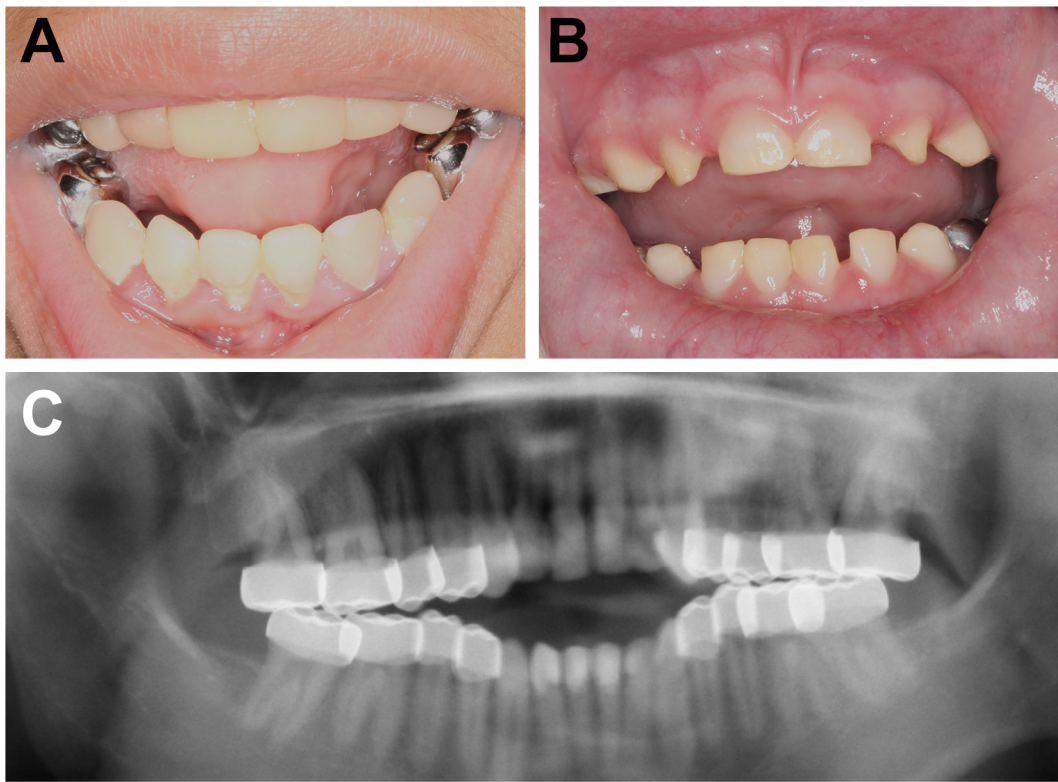


Figure2-Dental.tif